Applied Catalysis B: Environmental 183 (2016) 263–268

Contents lists available at ScienceDirect

Applied Catalysis B: Environmental

journal homepage: www.elsevier.com/locate/apcatb

Photodegradation of phenol via C_3N_4-agar hybrid hydrogel 3D photocatalysts with free separation

Mo Zhang [a,b], Wenjun Jiang [a], Di Liu [a], Jun Wang [a], Yanfang Liu [a], Yanyan Zhu [a], Yongfa Zhu [a,*]

[a] Beijing Key Laboratory for Analytical Methods and Instrumentation, Tsinghua University, Beijing 100084, China
[b] Department of Biophysics and Structural Biology, Institute of Basic Medical Sciences, Chinese Academy of Medical Sciences & School of Basic Medicine, Peking Union Medical College, Beijing 100730, China

ARTICLE INFO

Article history:
Received 8 September 2015
Received in revised form 22 October 2015
Accepted 24 October 2015
Available online 30 October 2015

Keywords:
$g\text{-}C_3N_4$
Agar
Hybrid hydrogel
Photocatalysis

ABSTRACT

The agar-C_3N_4 hybrid hydrogel photocatalysts with 3 dimension (3D) network structure have been prepared via thermoreversible phase transition of agar. The hybrid hydrogels show high efficient pollutants removal ability by synergistic effect of adsorption and photocatalytic degradation. The removal ability of phenol and methylene blue (MB) by hybrid hydrogel is about 1.3 and 4.5 times of pure $g\text{-}C_3N_4$ respectively. The pollution can be degraded continuously via agar-C_3N_4 hybrid hydrogels photocatalysts without separation.

1. Introduction

Recently, the problems of environmental pollution have become increasingly serious, posing a great threat to human health and sustainable development [1–6]. A lot of efforts have been made to remove the organic pollution in water, such as adsorption [7], photocatalytic degradation [8,9], biological treatment [10] and so on. The adsorption is one of the most widely used methods because of the high adsorption efficiency and low cost of the adsorption materials [11–14]. Among all the adsorption materials, the 3D hydrogels have attracted much attention due to their outstanding performance of adsorption and concentration of water pollutants [15–18]. On the one hand, the adsorption materials with three-dimensional network structure avoid aggregation and provide convenient mass transfer channels. On the other hand, the bulk structure can prevent the materials from dispersing in water [19–22]. The operation, collection and separation of the materials from water are simplified by a wide margin. However, the application of 3D hydrogels is limited by their disadvantages. The organic pollutants just can be concentrated rather than degraded to non-polluting molecules by hydrogels. The pollution problem cannot be solved drastically. Besides, only the materials undergo tedious desorption process can they be recycled. Therefore, materials with both ability of pollutants adsorption and degradation are undoubtedly the most advantageous.

Graphic carbon nitride ($g\text{-}C_3N_4$) is an attractive organic semiconductor photocatalyst with visible light activity and excellent thermal and chemical stability [23–25]. It has attracted extensive attention in degradation of organic pollutants, production of H_2 and O_2 from water and photocatalytic conversion of CO_2 under visible light [24,26–28]. However, the catalytic activity of $g\text{-}C_3N_4$ is limited by its poor adsorption ability for some pollutants, such as phenol. Moreover, it is difficult for the nano-sized $g\text{-}C_3N_4$ particles to be separated from water completely. Thus, novel $g\text{-}C_3N_4$ based hybrid hydrogels is not only facile to be separated from water to avoid secondary pollution, but also likely to show improved pollutants removal ability by synergistic effect of adsorption and photocatalytic degradation.

As a biopolymer gel, agar is widely used in the preparation of culture medium and polymeric hybrid hydrogels [29–31]. The application of agar in catalysis field has not been reported yet. In this paper, agar is used to prepare hybrid hydrogels via its thermoreversible sol–gel transition (Scheme 1). Agar and $g\text{-}C_3N_4$ nano-particle hydrosol is transformed into hybrid hydrogel with 3D network structure by a heating–cooling polymerization process. The agar-C_3N_4 hybrid hydrogels show enhanced performance

* Corresponding author. Fax: +86-010-62787601.
E-mail address: zhuyf@mail.tsinghua.edu.cn (Y. Zhu).

http://dx.doi.org/10.1016/j.apcatb.2015.10.049
0926-3373/

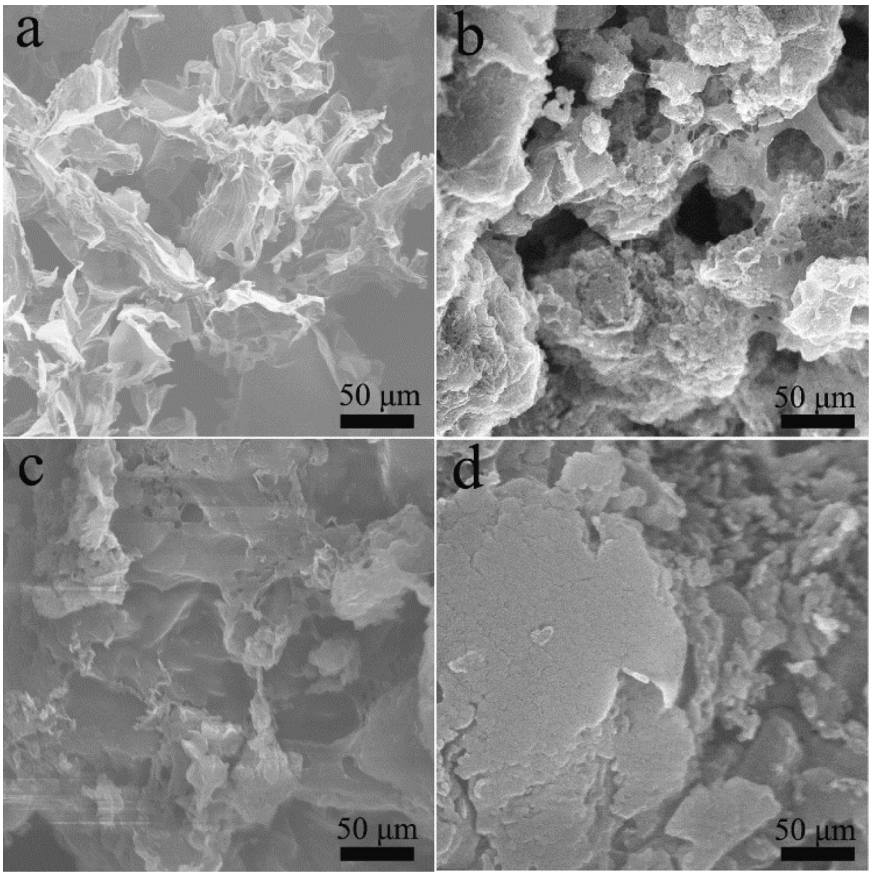

Fig. 1. The SEM images of pure agar (a) pure C_3N_4 (d) and C_3N_4-agar hybrid hydrogels (40% and 90%, b and c).

in photocatalytic degradation of MB and phenol under visible light via synergistic effect of adsorption and photocatalysis. The hybrid hydrogel exhibits excellent cyclic stability and can be used continuously without adsorption saturation. The C_3N_4-agar hybrid hydrogels are promising materials used in the treatment of water pollutants.

2. Experimental

2.1. Preparation of the C_3N_4-agar hybrid hydrogels

Agar and dicyandiamide were purchased from Sinopharm Chemical Reagent Corp., PR China. All other reagents used in this research were analytically pure and used without further purification.

The g-C_3N_4 was prepared by pyrolysis of dicyandiamide in air atmosphere. The typical preparation of g-C_3N_4 photocatalysts was as follows: The dicyandiamide was put in a Muffle Furnace and heated to 550 °C for 4 h to complete the reaction. The yield of the optimum g-C_3N_4 was about 25%.

Agar and g-C_3N_4 nano-particle hydrosol is transformed into hybrid hydrogel with 3D network structure by a heating–cooling polymerization process. The typical preparation process was as follows: A certain proportion of agar and g-C_3N_4 were put in to water and dispersed by ultrasound for 30 min. The hydrosol of mixture was heated up to 95 °C for 5 min and then cooled to room temperature in air to form C_3N_4-agar hybrid hydrogel. The 60%-TiO_2-agar was prepared by the similar method. 300 mg TiO_2 and 200 mg agar were put into water and ultrasound for 30 min. The hydrosol of mixture was heated up to 95 °C for 5 min and then cooled to room temperature in air to form 60%-TiO_2-agar hybrid hydrogel.

2.2. Characterizations

The morphologies and structure of the C_3N_4-agar hybrid hydrogels were characterized by a Hitachi SU-8010 Field Emission Gun Scanning Electron Microscopy and a Hitachi HT 7700 electron microscope operated at an accelerating voltage of 100 kV. UV–vis diffuse reflectance spectroscopy (DRS) was examined by Hitachi U-3010 UV–vis spectrophotometer with $BaSO_4$ as the reference sample. The crystallinity of the hybrid hydrogels were characterized by X-ray diffraction (XRD) on Bruker D8-advance diffractometer using Cu-Kα radiation (λ = 1.5418 Å). Raman spectra were recorded on a microscopic confocal Raman spectrometer (HORIBA HR800) with an excitation of 785 nm laser light. Fourier transform infrared (FT-IR) spectra were carried out using Bruker V70 spectrometer in the frequency of 4000–600 cm^{-1} with a resolution of 1 cm^{-1}. The photocurrents were measured on an electrochemical system (CHI 660B, China). Visible light was obtained from a 500 W xenon lamp (Institute for Electric Light Sources, Beijing) with a 420 nm cutoff filter.

2.3. Photocatalytic experiments

The synergistic effect of adsorption and photocatalytic degradation of the hybrid hydrogels in static systems were evaluated by the decomposition of MB and phenol solution in multi-tube agitated reactor (XPA-7). Visible light source was obtained by a 500 W Xe lamp (Institute for Electric Light Sources, Beijing) with a 420 nm cutoff filter, and the average visible light intensity was 35 mW cm^{-2}. 25 mg photocatalyst was added into prepared 50 mL 3×10^{-5} mol L^{-1} MB solution or 5 ppm phenol solution. The suspensions were magnetically stirred with visible light irradiation. At given time intervals, 3 mL aliquots were sampled and centrifuged

to remove the photocatalysts. The MB supernatant liquid was analysed by recording variations of the maximum absorption peak (664 nm for MB) using a Hitachi U-3010 UV–vis spectrophotometer. The chromatographic experiments with HPLC-UV/vis system were carried out using an ultraviolet absorbance detector (K 2501) operated at 275 nm coupled to a Venusil XBP-C_{18} (Agela Technologies Inc.) column. Before the analysis, the samples were filtered through Millipore discs of 0.45 μm to protect the chromatographic column. The mobile phase used for eluting phenol and its degradation intermediates from the HPLC columns consisted of methanol and water (60:40, v/v) at a flow rate of 1 mL min^{-1}.

The synergistic effect of adsorption and photocatalytic degradation of the hybrid hydrogels in dynamic systems were evaluated by the decomposition of MB in a home-made quartz reactor. 200 mg photocatalyst was coated on the rectangular Ni mesh (4 cm × 5.5 cm). The fresh liquid flows through the reactor by a pump. The diameter of the reactor is 9 cm, the liquid level is 1 cm from the bottom of the reactor, rectangular Ni mesh is 0.5 cm from the bottom of the reactor and the volume of the liquid in the reactor is 65 mL. At given time intervals, 2 mL aliquots were sampled from the lower right corner of the reactor. The aliquots did not need to be centrifuged and were directly analysed by recording variations of the maximum absorption peak (664 nm for MB) using a Hitachi U-3010 UV–vis spectrophotometer.

3. Results and discussion

The agar sol can transform to gel rapidly due to its coil–helix structural transition between high (90–95 °C) and low temperature. As shown in Fig. S1, the 90%-agar-C_3N_4 hybrid hydrogel shows negligible weight loss under the UV irradiation for 1000 h. However, the 60%-agar-TiO_2 hybrid hydrogel shows about 30% weight loss under the same conditions. The mass stability indicate that agar hybrid hydrogel maintained light stability with mild g-C_3N_4 photocatalyst but may be degradated by materials with high mineralization ability, such as TiO_2.

The agar hydrogel exhibits 3D network structure with crosslinked agar microsheets (Fig. 1). As shown in the SEM images, with the introduction of g-C_3N_4, the g-C_3N_4 is coated by agar uniformly and forms mutual crosslinking network. With increasing g-C_3N_4 content, the network structure of the hybrid hydrogel is less obvious. The pure g-C_3N_4 exhibits bulk morphology. The structures of hybrid hydrogels can be further proved by their TEM images in Fig. S2. The agar hydrogel is linked with each other and wrapped with g-C_3N_4, as the link bridge of g-C_3N_4 particles.

As shown in the X-ray diffraction (XRD) patterns (Fig. S3), agar is amorphous without obvious XRD peak. With increasing g-C_3N_4 content, the hybrid hydrogels give two peaks at 13.1° (1 0 0) and 27.5° (0 0 2) consistent with pure g-C_3N_4, corresponding to the in-plane ordering of tri-*s*-triazine units and graphitic structure of g-C_3N_4 [32]. The peak intensities are enhanced with the increasing g-C_3N_4 content, indicating the same crystal structure and higher structure order with large amounts of g-C_3N_4.

The structure of hybrid hydrogels can be further confirmed by FTIR and Raman spectra. As shown in Fig. S4, the characteristic bands at 1200–1600 cm^{-1} and 806 cm^{-1} are sharper with increasing g-C_3N_4 content, which are attributed to the stretching of aromatic CN heterocycle and the breathing of the triazine unit [33]. Thus, the bands of agar at 1050 cm^{-1} and 3000–3600 cm^{-1} originated from C—O and O—H [34] are getting subtle with large amounts of g-C_3N_4. In addition, the characteristic Raman spectra (Fig. S5) of hybrid hydrogels are similar to that of pure g-C_3N_4. The shaper bands are attributed to more ordered packing of g-C_3N_4 with increasing g-C_3N_4 content, which is consistent with the results

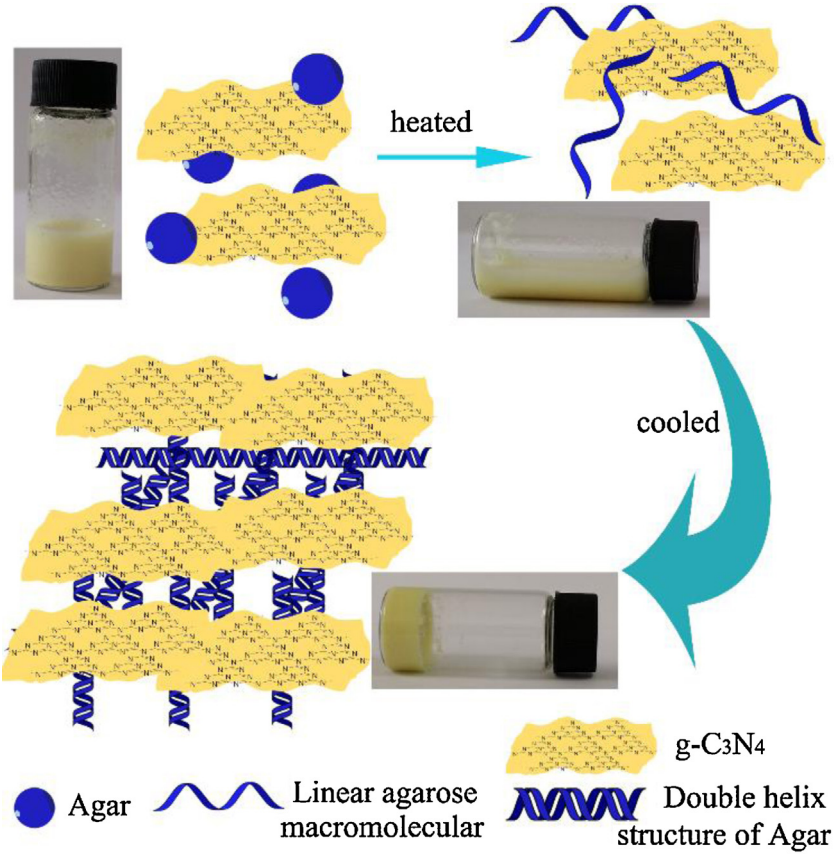

Scheme 1. Schematic illustration of preparation of C_3N_4-agar hybrid hydrogel.

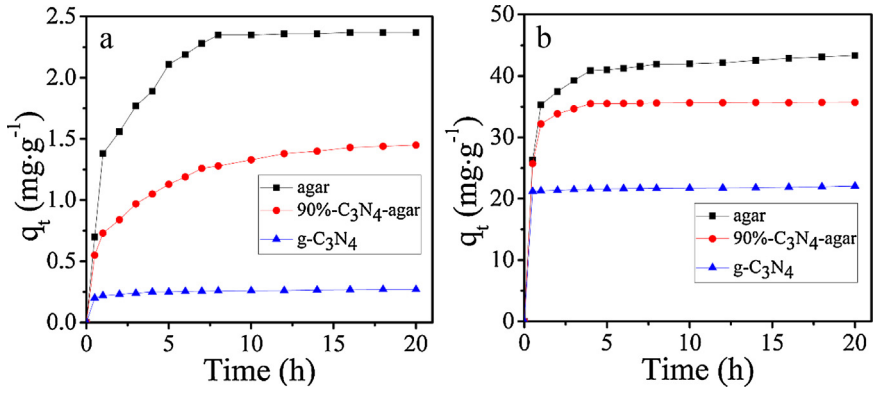

Fig. 2. Adsorption of phenol (a) and MB (b) by agar hydrogel, g-C_3N_4 and C_3N_4-agar hybrid hydrogels.

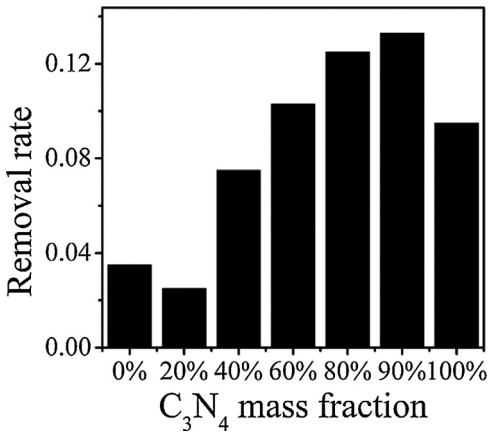

Fig. 3. The phenol removal rate by agar aerogel, hybrid aerogel and pure g-C_3N_4 via synergistic effect of adsorption and photocatalytic degradation in static systems.

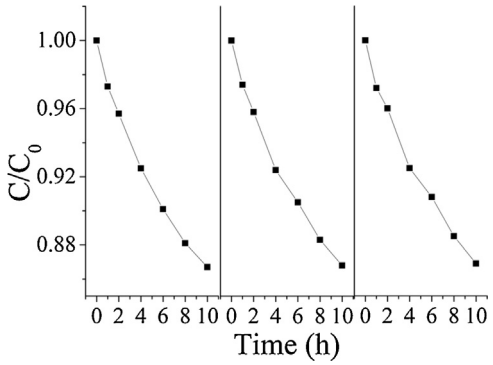

Fig. 4. The cycling stability of 90%-C_3N_4-agar hybrid aerogel for phenol removal.

of XRD and FTIR. The UV–vis reflectance spectra in Fig. S6 shows an obvious absorption red shift of hybrid hydrogels from 460 to 490 nm with introduction of agar compared to g-C_3N_4, indicating the extended absorption of C_3N_4-agar in visible light region.

The zeta potentials of hybrid hydrogels (Fig. S7) measured in aqueous solutions at pH 6.5 were between −50 and −58 eV, indicating ample stability of the materials in the condition. The adsorption capacity of agar aerogel, 90%-C_3N_4-agar hybrid aerogel and pure g-C_3N_4 are compared by equilibrium adsorption isotherm studies in Fig. 2. As shown in Fig. 2, the adsorption capacities of 90%-C_3N_4-agar hybrid aerogel are about 1.3 and 35 mg g^{-1} for phenol and MB, which are 5.4 and 1.6 times as that of pure g-C_3N_4. The agar aerogel performs the best adsorption capacity.

The agar-C_3N_4 hybrid aerogels exhibit enhanced performance in pollutants removal, such as phenol and MB. As shown in Fig. S8, the pure agar aerogel performs better adsorption capacity of phenol than hybrid aerogel and pure g-C_3N_4 in the first two hours. However, the agar cannot remove the pollutants after the adsorption equilibrium reached in 5 h. The hybrid aerogels with low g-C_3N_4 content (20–60%) perform less adsorption capacity and photocatalytic degradation ability, leading to their less pollutants removal ability. With obvious adsorption capacity and photocatalytic degradation ability at the same time, the 80% and 90%-C_3N_4-agar hybrid aerogels enhanced performance in pollutants removal via synergistic effect of adsorption and photocatalytic degradation, which is 1.3 times as that of pure g-C_3N_4 (Fig. 3). More importantly, the hybrid aerogel exhibits excellent cycling stability (Fig. 4) for phenol removal without tedious desorption and recovery process, which is attributed to its photocatalytic degradation ability and 3D bulk structure.

The variation trend of MB removal by hybrid aerogels is different from that of phenol. As shown in Fig. S9, the MB removal ability is decreased with increasing g-C_3N_4 content in 5 h, due to the much better MB adsorption capacity of agar than g-C_3N_4. It is observed that the degradation ability of 20% and 40%-C_3N_4-agar hybrid aerogels is not obvious after adsorption saturation, while 60–90% C_3N_4-agar hybrid aerogels perform enhanced degradation ability.

To investigate the synergy of MB adsorption and photocatalytic degradation by hybrid hydrogel, a long-time detection in dynamic system is designed. As shown in Fig. 5a, the concentration of MB effluent liquid decreases quickly with continuous fresh MB solution through the pure agar and hybrid hydrogel in 4 h, due to their excellent adsorption capacity of MB compared with g-C_3N_4. However, concentration of MB effluent liquid through pure agar hydrogel reaches the initial value in the later 6 h since the adsorption equilibrium is reached. With synergy of adsorption and photocatalytic degradation, MB can be removed by 90%-C_3N_4-agar hybrid hydrogel continuously (Fig. 5b). The removal efficiency of MB by hybrid hydrogel is 4.5 times as that of pure g-C_3N_4. Therefore, with the advantage of hydrogel, the C_3N_4-agar hybrid hydrogels exhibit enhanced performance in adsorption and in situ degradation of organic pollutants and improved cycling stability as well.

The enhancement performance can be attribute to the synergy of adsorption and photocatalytic degradation of hybrid hydrogels with bulk 3D network structures. On the one hand, the structure can provide convenient mass transfer channels for adsorption and in situ degradation of organic pollutants. On the other hand, the bulk structure can avoid aggregation of g-C_3N_4 and prevent them from dispersing in water, greatly simplifying the collection and separation of g-C_3N_4 from water. Although the visible performance enhancement of g-C_3N_4 for phenol and MB degradation may not be remarkable as other hybrid materials based on g-C_3N_4, the 3D

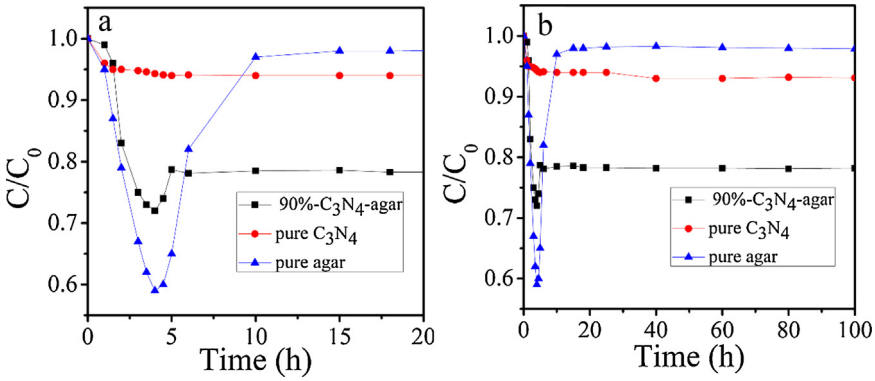

Fig. 5. The MB removal abilities of agar aerogel, hybrid aerogel and pure g-C_3N_4 via synergistic effect of adsorption and photocatalytic degradation in dynamic system for 20 (a) and 100 (b) hours.

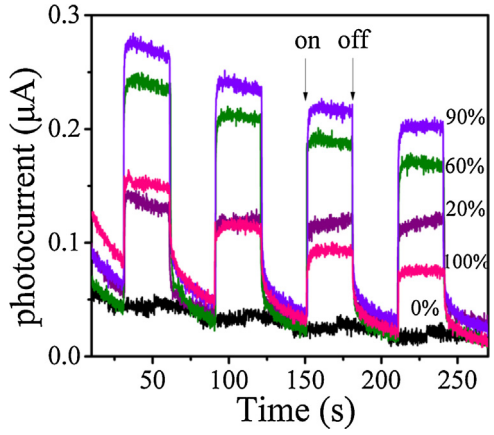

Fig. 6. The photocurrent of agar aerogel, hybrid aerogel and pure g-C_3N_4.

network structures and free-separation characteristic of agar-C_3N_4 hybrid hydrogels determined their wide application prospect in water pollution treatment.

The synergy of adsorption and photocatalytic degradation by hybrid hydrogel is further explored by photocurrent. As shown in Fig. 6, little photoelectric response of agar can be observed. The photocurrent of 20%-C_3N_4-agar is similar to that of pure g-C_3N_4, while 40–90% materials perform enhanced photoelectric response. The enhanced photocurrent of hybrid hydrogels may due to the improved transition of photogenerated carriers via the porous network structure, which is consistent with the results of phenol degradation. Thus, in addition to the adsorption capacity, the photogenerated carriers' mobility of hybrid hydrogels can also be enhanced by their 3D network structure, leading to their dramatically enhanced pollutants removal ability.

4. Conclusion

In conclusion, the series agar-C_3N_4 hybrid hydrogels are prepared by a heating–cooling polymerization method. The C_3N_4-agar hybrid hydrogels show enhanced performance in photocatalytic degradation of phenol and MB under visible light via synergistic effect of adsorption and photocatalysis. The removal of phenol and methylene by optimal hybrid hydrogel is about 1.3 and 4.5 times of pure g-C_3N_4 respectively. The hybrid hydrogel exhibits excellent cyclic stability and can be used for long time. The C_3N_4-agar hybrid hydrogels are promising materials used in the treatment of water pollutants.

Acknowledgments

This work was partly supported by National Basic Research Program of China (973 Program) (2013CB632403), National High Technology Research and Development Program of China (2012AA062701) and Chinese National Science Foundation (21437003, and 21373121).

Appendix A. Supplementary data

Supplementary data associated with this article can be found, in the online version, at http://dx.doi.org/10.1016/j.apcatb.2015.10.049.

References

[1] M.A. Shannon, P.W. Bohn, M. Elimelech, J.G. Georgiadis, B.J. Marinas, A.M. Mayes, Nature 452 (2008) 301–310.
[2] H. Lee, J. Choi, S. Lee, S.T. Yun, C. Lee, J. Lee, Appl. Catal. B Environ. 138–139 (2013) 311–317.
[3] G.S. Shao, X.J. Zhang, Z.Y. Yuan, Appl. Catal. B Environ. 82 (2008) 208–218.
[4] M. Zhou, J. Yu, S.P. Liu Zhai, B. Huang, Appl. Catal. B Environ. 89 (2009) 160–166.
[5] C. Gebald, J.A. Wurzbacher, P. Tingaut, T. Zimmermann, A. Steinfeld, Environ. Sci. Technol. 45 (2011) 9101–9108.
[6] M.S. Mauter, M. Elimelech, Environ. Sci. Technol. 42 (2008) 5843–5859.
[7] J. Xu, L. Wang, Y. Zhu, Langmuir 28 (2012) 8418–8425.
[8] Y. Wang, R. Shi, J. Lin, Y. Zhu, Energy Environ. Sci. 4 (2011) 2922–2929.
[9] M.M. Khin, A.S. Nair, V.J. Babu, R. Murugan, S. Ramakrishna, Energy Environ. Sci. 5 (2012) 8075–8109.
[10] F. Yamaga, K. Washio, M. Morikawa, Environ. Sci. Technol. 44 (2010) 6470–6474.
[11] S.K. Parida, S. Dash, S. Patel, B.K. Mishra, Adv. Colloid Interfaces 121 (2006) 77–110.
[12] T.F. Lin, J.K. Wu, Water Res. 35 (2001) 2049–2057.
[13] B. Pan, B. Pan, W. Zhang, L. Lv, Q. Zhang, S. Zheng, Chem. Eng. J. 151 (2009) 19–29.
[14] G. Mezohegyi, F.P. van der Zee, J. Font, A. Fortuny, A. Fabregat, J. Environ. Manage. 102 (2012) 148–164.
[15] Y. Chen, L. Chen, H. Bai, L. Li, J. Mater. Chem. A 1 (2013) 1992–2001.
[16] Z. Sui, Q. Meng, X. Zhang, R. Ma, B. Cao, J. Mater. Chem. 22 (2012) 8767–8771.
[17] S. Babel, T.A. Kurniawan, J. Hazard. Mater. 97 (2003) 219–243.
[18] H. Gao, Y. Sun, J. Zhou, R. Xu, H. Duan, Acs Appl. Mater. Interfaces 5 (2013) 425–432.
[19] G. Crini, Bioresour. Technol. 97 (2006) 1061–1085.
[20] S. Liu, A. Tang, M. Xie, Y. Zhao, J. Jiang, G. Liang, Angew. Chem. Int. Ed. 54 (2015) 3639–3642.
[21] X. Gao, R.J. Esteves, T.T.H. Luong, R. Jaini, I.U. Arachchige, J. Am. Chem. Soc. 136 (2014) 7993–8002.
[22] D.S. Franklin, S. Guhanathan, J. Appl. Polym. Sci. 132 (2015), http://dx.doi.org/10.1002/app.41921.
[23] X. Wang, K. Maeda, A. Thomas, K. Takanabe, G. Xin, J.M. Carlsson, K. Domen, M. Antonietti, Nat. Mater. 8 (2009) 76–80.
[24] X. Wang, S. Blechert, M. Antonietti, ACS Catal. 2 (2012) 1596–1606.
[25] P. Niu, L.L. Zhang, G. Liu, H.M. Cheng, Adv. Funct. Mater. 22 (2012) 4763–4770.
[26] Y. Zheng, J. Liu, J. Liang, M. Jaroniec, S.Z. Qiao, Energy Environ. Sci. 5 (2012) 6717–6731.

[27] Y. Zhao, F. Zhao, X. Wang, C. Xu, Z. Zhang, G. Shi, L. Qu, Angew. Chem. Int. Ed. 53 (2014) 13934–13939.
[28] Y. He, L. Zhang, B. Teng, M. Fan, Environ. Sci. Technol. 49 (2015) 649–656.
[29] S. Pradhan, P. Patra, S. Mitra, K.K. Dey, S. Basu, S. Chandra, P. Palit, A. Goswami, J. Agric. Food Chem. 63 (2015) 2606–2617.
[30] K. Vukoti, X. Yu, Q. Sheng, S. Saha, Z. Feng, A.L. Hsu, M. Miyagi, J Proteome Res. 14 (2015) 1483–1494.
[31] Q. Chen, L. Zhu, C. Zhao, Q. Wang, J. Zheng, Adv. Mater. 25 (2013) 4171–4176.
[32] X. Wang, X. Chen, A. Thomas, X. Fu, M. Antonietti, Adv. Mater. 21 (2009) 1609–1612.
[33] A. Vinu, K. Ariga, T. Mori, T. Nakanishi, S. Hishita, D. Golberg, Y. Bando, Adv. Mater. 17 (2005) 1648–1652.
[34] M.P. Santoro Marchetti, F. Rossi, G. Perale, F. Castiglione, A. Mele, M. Masi, J. Phys. Chem. B 115 (2011) 2503–2510.